

Optimizing Millimeter-Wave Backhaul Networks in Roadside Environments

Qiang Hu and Douglas M. Blough

School of Electrical and Computer Engineering, Georgia Institute of Technology

Abstract—With the advent of 5G, mmWave communications are being investigated for wireless backhaul. The high data rates possible with mmWave are well suited for backhaul networks, while the large number of small cells necessary to support 5G make connecting fiber to every base station difficult and costly. We investigate backhaul topologies deployed along roadsides to provide 5G service to vehicles. The challenge is to achieve the very high data rates necessary to handle backhaul traffic while managing self interference that can occur due to the near-straight-line topology that arises from a roadside deployment. We investigate wireless backhaul networks that use relay nodes and a regular triangular-wave topology to meet the performance objective. The triangular-wave is a regular topology that can be deployed on regularly-spaced lampposts alongside a road. We derive conditions necessary for the triangular-wave topology to be interference-free and throughput-optimal. We also investigate how the proposed topology performs using lamppost positions taken from a 12 km stretch of highway in Atlanta. Results show that the topology can achieve throughputs very close to the ideal case and is capable of supporting backhaul throughputs of 10+ Gbps in real roadside environments.

I. INTRODUCTION

Research is well underway toward development of 5G wireless networks based on millimeter wave (mmWave) communication [1]. mmWave has the potential to provide ultra high speed wireless communication to support 5G applications but it also has some undesirable characteristics that have to be mitigated for the 5G vision to become reality. These include higher path loss, higher oxygen and H₂O absorption [2], and greater susceptibility to blockages [3], as compared to the lower-frequency signals used in today's WiFi and cellular networks. These signal propagation issues limit the communication range for very high rate mmWave links to several hundred meters and necessitate the use of small cells to connect users to the network. A typical small cell has a radius of a few hundred meters as compared to today's macro cells, which have radii of several miles. Another characteristic feature of mmWave communication is the use of very narrow beamwidth, high gain directional antennas, which can integrate large numbers of antenna array elements closely together due to the much shorter wavelengths of mmWave signals. This helps alleviate signal propagation problems and reduces the interference footprint of mmWave links.

The demand for high-speed wireless communications in vehicles, e.g. video streaming for the entertainment of vehicle passengers, is rapidly increasing. Given the small cells that will be used in 5G and increased demand from vehicles, it is very likely that many base stations (BSs) will need to be placed very close to roadways, e.g. highways. This will be true in heavily trafficked road sections even outside of

major urban areas. Connecting fiber backhaul networks to such roadside networks will be costly and difficult, and therefore it is expected that wireless backhaul networks will be used in segments to connect to a limited number of network nodes having fiber connections. mmWave communication is the most attractive candidate for wireless backhaul due to its ability to support very high data rates.

mmWave backhaul is also being proposed for use in urban areas [4]. However, in urban environments, interference between different mmWave links is almost completely eliminated due to the presence of many large obstacles [12]. In more wide open areas, such as along roadsides or in rural areas,¹ interference is not limited by obstacles and must be taken into account when designing the backhaul network. Even though the interference footprint is reduced due to the use of narrow beamwidth directional antennas, concurrent transmissions of multiple links along a network path may cause mutual interference, because the beam directions of all antennas are close to the road direction. We show later that, without specific arrangement and coordination, mutual interference greatly reduces link capacity in this setting.

In this paper, we investigate the design of interference-free and throughput-optimal mmWave backhaul topologies that can be deployed along a roadside, e.g. by mounting nodes on regularly-spaced lampposts that are already present on most roads and highways. We propose and analyze the triangular-wave topology, which is a regular topology well-suited for this problem setting. We first derive the conditions necessary for the triangular-wave topology to produce interference-free transmissions that can be easily and optimally scheduled. For a given antenna beamwidth, we also derive conditions on the height and spacing of lampposts that are necessary to support an interference-free triangular-wave topology and show that, if these conditions are satisfied, the topology is throughput optimal. We also investigate how well the proposed topology performs using actual lamppost positions taken from a 12 km stretch of highway in Atlanta using Google Earth. The results show that the proposed topology can achieve network throughputs very close to the ideal case and can support backhaul throughputs of 10+ Gbps in real roadside scenarios.

II. RELATED WORK

A number of different issues related to mmWave backhaul networks in dense urban environments have been investigated.

¹Some of the work described in this paper could be useful in rural backhaul deployments also. However, in the remainder of the paper, we focus solely on roadside network deployments.

In [4], a point-to-multipoint inband mmWave backhaul with TDMA-based scheduling for urban environments is proposed and analyzed. In [5], the rate distribution for mmWave networks in urban environments is characterized through a model that captures the key features of narrow-beam directional antennas and resource sharing between access and backhaul network links. Finally, in [6], a QoS-aware scheduling algorithm that aims to maximize the number of flows having their QoS requirements satisfied in a mmWave backhaul network is presented and evaluated.

The work described above differs from ours in several important ways. First, it assumes the backhaul network covers cells that are spread across a broad geographic area and the backhaul topology is either a tree or a mesh network. In the roadside deployments we consider herein, cells cover a more or less linear area that follows the roadway and the network topology is therefore a simple path. Second, as shown in [12], interference can be largely ignored for mmWave in the general urban environment due to the use of narrow beamwidth directional antennas and the presence of many large obstacles. However, in roadside deployments that are largely free of obstacles with transmissions that are all in the same general direction, interference must be considered. We develop topologies that can eliminate interference and achieve significantly higher throughput than interference-unaware topologies.

There is one work that considers a street deployment of cells [7], where the authors jointly optimize the topology, power and bandwidth allocation for a “street canyon” scenario. However, this work assumes that the carrier frequencies of different links are orthogonal to one another and, therefore, interference is not considered. In our work, the same frequency band is used by all mmWave backhaul links but interference is eliminated. The use of a different carrier frequency for every link in a backhaul path unnecessarily divides the bandwidth of the wireless channel and, therefore, results in lower throughput than using a single frequency that can use the full bandwidth of the channel on every link.

Our work makes use of relay nodes to ensure that link capacities can support the intensive backhaul traffic requirements. Relays have been studied in other mmWave contexts as well. The placement and selection of a single relay for WPANs and the corresponding scheduling problem have been addressed [8]–[10]. These works only consider the indoor deployment of a single relay while in our work multiple relays are deployed in the outdoor roadside scenario to build a larger mmWave backhaul network. Use of single relays has also been considered in the outdoor mmWave environment to enhance network coverage and capacity [11].

III. RELAY-ASSISTED MMWAVE BACKHAUL ON ROADSIDES

In the 5G era, mmWave small cell BSs will be deployed along roads and highways to provide ultra high speed data service for communications with vehicles. mmWave small cells in dense urban environments can only sustain a radius of around 100 meters due to the presence of many obstacles. However, in a roadside deployment, a mmWave small cell

BS should be able to easily support a radius of at least 500 meters, because of the relatively obstacle-free environment. This means a BS separation of 1 km is sufficient to provide full coverage to the roadway and the length of a self-backhaul link will then be about 1 km. In Fig. 1, we can see that a mmWave link with 1 km length at 60 GHz can reach a capacity of around 0.9 Gbps². We assume that the relationship between SNR and

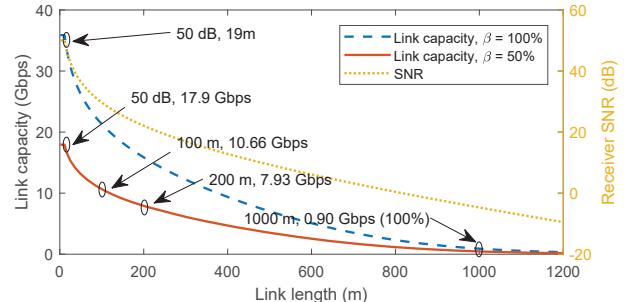


Fig. 1. mmWave link capacity against link length

link capacity obeys the well-known Shannon equation,

$$C = B \log_2(1 + \min\{\text{SNR}, T_{max}\}) , \quad (1)$$

where C is the link capacity, B is bandwidth, SNR is the signal-to-noise ratio, and T_{max} (e.g., 50 dB) is the SNR that produces the link’s maximum rate. In practice, capacity cannot be increased without limit and this is captured by T_{max} .

As mentioned above, mmWave small cell BSs are expected to be deployed about every 1 km along a roadway. Moreover, considering the cost of running fiber to small cell BSs, having a separation of around 10–20 km between anchored-BSs (A-BSs) that are wire-connected to the broader network is a reasonable assumption. We also assume that a single mmWave node cannot transmit and receive at the same time, commonly referred to as the *primary interference constraint*. Define the *link utility ratio* β as the percentage of time that a link is active out of the total time. Due to the primary constraint, backhaul links have a utility ratio of at most 50%, which halves the average throughput of a backhaul link (see Fig. 1). To deal with the high path loss in mmWave band, we assume that nodes are equipped with two high-gain directional antennas with narrow beamwidth, where one antenna is used to transmit and the other is used to receive.

A. mmWave self-backhaul in a “straight-line” topology

A segment of a roadside mmWave backhaul network is shown in Fig. 2 with small cell BSs mounted on the tops of lampposts. Lamppost mounting provides easy access to power, good access tier coverage for vehicles on the road, and ease of deployment. Adjacent BSs are connected by mmWave backhaul links (shown in red), which use beamforming to achieve signal directionality. The left-most BS, also shown in red, has a fiber connection to the Internet, thus it is an A-BS. Fig. 2 shows one simple traffic pattern in the backhaul network, where data is disseminated from left to right (i.e., from B_0 to $B_1 \dots B_{10}$), or data is aggregated from right

²The detailed simulation setting can be found in Section V.

to left. All data is consumed/generated by vehicles on the road and the access tier links operate on a different frequency from the backhaul links. Obviously, the left-most backhaul link (B_0, B_1) has the largest traffic load of about 10 Gbps.

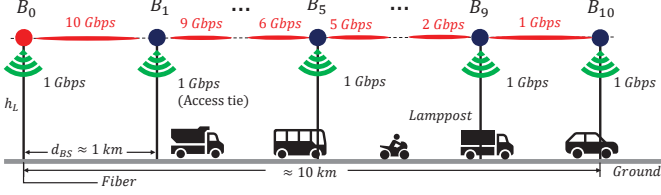


Fig. 2. A segment of a mmWave backhaul network along a roadway

The “straight-line” topology for *self-backhaul* is simple but it has two issues that prevent it from achieving high throughput. First, the link length is around 1 km which is too long to support more than 1 Gbps traffic as shown in Fig. 1. Second, the signal directions for the antennas on a sequence of BSs are colinear, which will cause severe mutual interference leading to poor system throughput when concurrent transmissions occur on multiple links. In [7], all backhaul links use orthogonal frequency bands to get rid of mutual interference in a street canyon scenario, however the system can only support 4 hops with the access tier data rate at 1 Gbps and hop distance of 200m. The system capacity is limited to 3-4 Gbps, because it does not fully use the frequency resource. We introduce relays to the backhaul network and show that, through optimizing the relay placement and scheduling, both issues are resolved and a 10+ Gbps throughput objective can be met.

B. “Triangular-wave” topology for relay-aided backhaul

As mentioned above, deploying relays can resolve the two issues impeding the performance of straight-line networks without relays. With relays in between BSs, the length of each hop shrinks, which results in a higher single hop data rate. However, the introduction of relays raises two new issues: how to place relays and how to schedule the transmissions of relay links. If relays are still mounted on the top of lampposts following the “straight-line” topology, the backhaul network performance will still be poor due to the mutual interference. To eliminate mutual interference, we propose to deploy relays using a “triangular-wave” topology, as shown in either Fig. 3 or Fig. 4. In Fig. 3, all BSs and relays are deployed on the same side of the road in case the road only has lampposts on one side or in the median. If lampposts are present on both sides of a road, we can deploy relays according to Fig. 4.

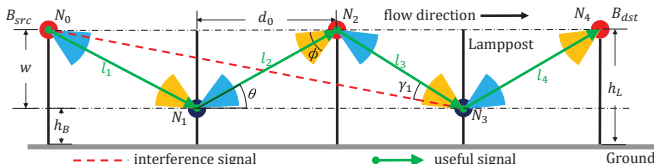


Fig. 3. A segment of relay-aided mmWave backhaul (one side)

In the “one-side” case, BSs are mounted on the top of lampposts with a height denoted by h_L . The BS on the left-

most lamppost is the source node, denoted as B_{src} (also as N_0 in Fig. 3). As shown in Fig. 3, the separation between consecutive lampposts that host a relay is d_0 . A destination BS, denoted as B_{dst} (also as N_5), is mounted on the top of the right-most lamppost. The first relay N_1 to the right of B_{src} is mounted at a specific height denoted as h_B where $h_B < h_L$. The next relay along the road N_2 is mounted on the top of the lamppost which is d_0 away from the lamppost hosting N_1 . From N_1 , every $2d_0$ there is one relay deployed at height h_B , while from N_2 , every $2d_0$ there is one relay mounted at height h_L , and this forms the so called “triangular wave” topology. Fig. 3 shows an example of 3 relays deployed between two adjacent BSs along the road. It is expected that in the “one-side” case, an odd number of relays are deployed between two adjacent BSs. When an even number of relays have to be deployed, an extra relay deployed at the height h_B on the same lamppost where B_{dst} is mounted could help to maintain the consistency of the triangular wave topology with a wired connection established between B_{dst} and the extra relay. Due to page limitations and the similarity of the analyses for the one-side and two-side cases, we focus on the one-side case in the remainder of the paper.

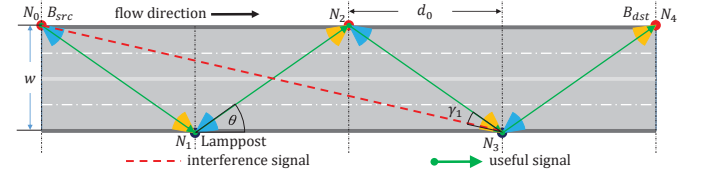


Fig. 4. A segment of relay-aided mmWave backhaul (two sides)

Note that, due to the static nature of the backhaul network, when wireless nodes are deployed, the beams of two adjacent nodes connected by a link are assumed to be aligned perfectly. The blue and orange beams represent transmit and receive beams respectively, and the beamwidth is denoted by ϕ . The angle θ depicted in the figures, e.g., $N_3\hat{N}_1N_2$, is referred to as the angle of elevation. d_0 and θ together determine the triangular-wave topology. We also refer to the even nodes as Group₀ nodes and the odd nodes as Group₁ nodes.

C. Different cases of mutual interference

The following analysis adopts the *flat-top* antenna model, in which the measured antenna gain $G(\alpha)$ is shown in Eq. 2, where α is the angle to the antenna boresight, $G_h \gg G_l$.

$$G(\alpha) = \begin{cases} G_h & \text{if } \alpha < \frac{\phi}{2} \\ G_l & \text{if } \alpha \geq \frac{\phi}{2} \end{cases} \quad (2)$$

Fig. 5 shows three different interference cases due to the possible position relationship between the intended link and the interfering link: (a) depicts the most interference case where the interference signal experiences G_h at both Tx_1 and Rx_2 . In (b), the antenna gains on interference signal are G_h and G_l , while in (c), both gains are G_l . If we assume the intended link length is 100 meters, an interferer is 300 meters away from the intended receiver, and $\beta = 50\%$, the achieved link rates are 0.72 Gbps, 6.91 Gbps, and 10.55 Gbps

in cases (a-c) respectively. Since in case (c), the amount of interference is smaller than the noise level, it is regarded as *interference-free*. The next subsection discusses the conditions under which the proposed triangular-wave topology can produce the interference-free case for all concurrently active links.

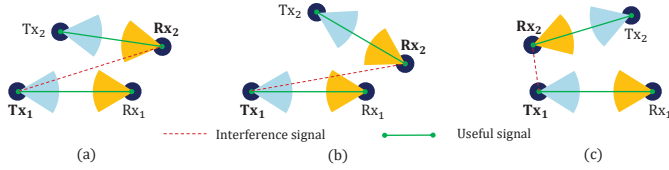


Fig. 5. Three different interference cases of two mmWave links

D. “Interference-free” condition for triangular-wave topology

As the angle θ decreases, the triangular-wave topology gets closer to the straight-line topology, which is more likely to encounter mutual interference. Also, when the beam width ϕ becomes smaller, it is more likely to generate an interference-free case given a fixed θ . Thus, it is intuitive to think that the conditions that enable interference-free communication in the triangular-wave topology are dependent on θ and ϕ .

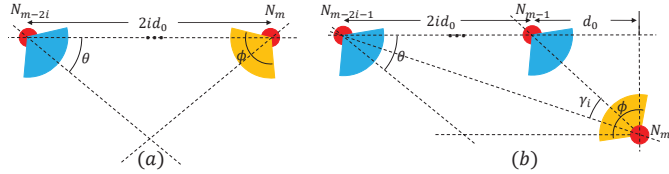


Fig. 6. Interfering (a) within the same group; (b) across different groups

As mentioned above, the nodes deployed in a mmWave backhaul with a triangular-wave topology can be partitioned into two groups (i.e., Group₀ and Group₁). Consider a node N_m ($3 \leq m \leq n$), as the receiving node of an intended link, where n is the total number of nodes in the backhaul network. The position relationship between the potential interferer node to N_m is depicted in Fig. 6. Fig. 6a shows the case where interferer N_{m-2i} ($m > 2i > 0$) comes from the same group as N_m . It is obvious that as long as $\theta < 0.5\phi$, N_{m-2i} 's transmission interferes with the reception of N_m . Fig. 6b depicts the scenario where interferer N_{m-2i-1} ($m > 2i + 1 > 0$) and receiver N_m are in different groups. If $\frac{\phi}{2} \leq \gamma_i$, N_{m-2i-1} does not interfere with N_m . Thus, the interference-free condition for the triangular-wave topology can be expressed as:

Theorem 1. The condition for an interference-free scenario in the triangular-wave topology is

$$\gamma_1 = \theta - \arctan\left(\frac{\tan\theta}{3}\right) \geq \frac{\phi}{2} \quad (3)$$

Proof. It is obvious that the first three nodes from the source end in the network will be interference free due to the primary constraint. As for the other nodes N_m , when $\theta < 90^\circ$, γ_i can be found as $\theta - \arctan\left(\frac{\tan\theta}{2i+1}\right)$, which monotonically increases as i increases. Thus, $\gamma_i > \gamma_1, i = 2, 3, \dots$, which means as long as Eq. 3 is satisfied, the nodes from different group will not interfere with N_m . In addition, since $\theta > \gamma_i$ is always

true, the nodes from the same group of N_m will not interfere N_m as well. Since the analysis can be applied to any node N_m in the network, Eq. 3 ensures that a receiver will not be interfered by any other node in the network. \square

Note that in the proof, we do not consider the potential interference caused by one-time reflections off the ground, because the potential reflected interference is controlled through optimal scheduling and topology design. Specifically, for the case shown in Fig. 6a, our optimal scheduling presented next will prevent the depicted transmitter and receiver from being active in the same time slot. For the case in Fig. 6b, since the receiving antenna of N_m is pointing up, the possible interference from a ground-reflected signal corresponds to the “single-gain” case as shown in Fig. 5b. However, due to the large reflection attenuation of mmWave signals (about 15 dB [13]), which is quite close to the antenna gain (e.g., 21.87 dBi in our simulation), the interference strength is close to the interference-free case (i.e., the interference level is smaller than the noise level). Thus the interference can still be ignored.

E. Optimal scheduling for triangular-wave topology

Due to the introduction of relays that produce multi-hop transmissions between consecutive BSs in the mmWave backhaul, link scheduling must be considered. We refer to the multi-hop path between a pair of BSs as a relay path. We assume that relay paths operate in TDMA fashion so that their performance can be maximized. We also assume that traffic flows in only one direction at a time across a given relay path.

If the relationship in Theorem 1 stands, a triangular wave deployment of mmWave backhaul is free-of-interference (i.e., interference is way smaller than the noise level). If thermal noise is considered and every node uses the same transmit power, the SNR value at every receiver is equal. Thus, the rates of all links are identical based on Eq. 1, and we denote that rate by R_{max} . We refer to the following schedule as the “by-2” schedule. There are two time slots of equal length in the schedule. In time slot 0, all even-numbered nodes transmit and in time slot 1, all odd-numbered nodes transmit.

Theorem 2. For interference-free triangular-wave topologies, the “by-2” schedule is optimal with a throughput of $R_{max}/2$.

The proof is straightforward and is omitted due to page limitations.

We will see in Section V that, given a typical highway scenario and with narrow beamwidth ($\phi \leq 15^\circ$), the throughput of a relay path can exceed 10 Gbps, which satisfies the requirement for backhaul in the highway scenario for future 5G networks. In the next section, we show that the triangular-wave topology is throughput-optimal under certain conditions.

IV. OPTIMALITY OF TRIANGULAR-WAVE TOPOLOGY

The triangular-wave topology has several advantages due to its symmetric deployment of relays and BSs along the highway. The links are the same length and, therefore, assuming the propagation environment is consistent along the road, the analysis of each link is identical, thereby reducing network

analysis complexity. The symmetric and homogeneous properties allow the analysis to be extended to any length of topology in a straightforward way. It also allows several virtual BS-to-BS long links to directly cascade together without mutual interference between them, which eases the network deployment. With symmetry, the analysis of the single-directional flow case can be easily applied to the reverse direction. It eases analysis of bi-directional flows (e.g., assigning time slots to the links in each direction by TDMA).

In addition to these practical advantages, it is possible to show that, if the lamppost configurations satisfy certain minimum conditions, the triangular-wave topology achieves the maximum end-to-end (i.e. BS-to-BS) throughput possible. These conditions are provided by Theorem 3.

Theorem 3. In the “one-side” deployment with at least 3 hops, given system parameters d_0 , h_L , and ϕ , select the minimum height h_B for relay deployment so that $\arctan(\frac{h_L-h_B}{d_0}) - \arctan(\frac{h_L-h_B}{3d_0}) = \frac{\phi}{2}$. Assume $d_0 = ah_L$, $a > 1$, if $h_B = b^{-1}h_L$, $b > 1$, and the following condition is satisfied,

$$\begin{cases} a > \sqrt{\frac{3(b-1)^3}{b^2(b-2)}} \\ b > 2 \end{cases} \quad (4)$$

the triangular-wave topology offers the largest end-to-end throughput among all possible topologies.

Proof. Based on Theorem 1, the selection of h_B guarantees that the triangular wave topology is interference-free. If a certain topology can outperform the triangular wave one, it must be interference-free as well, due to the great loss of link capacity in case mutual interference exists. Moreover, if a topology is interference-free and offers the maximum throughput, the “by-2” schedule is a necessity for it offers the largest link utility ratio. Hence, the theorem is proved if we can prove that given the proposed condition, any other topology requires a beam width ϕ' smaller than the given ϕ to achieve interference-free using the “by-2” schedule.

Consider a minimum segment with 4 nodes N_0 to N_3 deployed. N_0 is a BS mounted on the top of a lamppost, N_1 to N_3 can be deployed at any height within $[h_B, h_L]$. There are four possible interference-free scenarios when the “by-2” schedule is applied, as depicted in Fig. 7. Thus in this segment, N_0 must not interfere N_3 , when data flows from N_0 to N_3 .

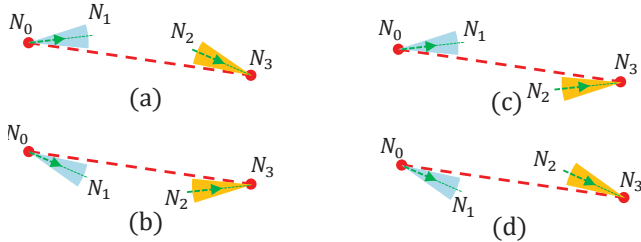


Fig. 7. Four possible interference-free scenarios.

As for case (a), to eliminate interference, the half beam width must be no larger than the largest possible angle $N_3\widehat{N_0}N_1$ and angle $N_0\widehat{N_3}N_2$. $N_3\widehat{N_0}N_1_{max} = \arctan(\frac{\tan\theta}{3})$

is obtained when N_1 and N_3 are at h_L and h_B , respectively. $N_0\widehat{N_3}N_2_{max} = \theta - \arctan(\frac{\tan\theta}{3})$ is achieved when N_2 and N_3 are at h_L and h_B , respectively. Thus, when $\theta < 60^\circ$,

$$\phi' \leq 2 \arctan(\frac{\tan\theta}{3}) < 2(\theta - \arctan(\frac{\tan\theta}{3})) \leq \phi \quad (5)$$

Similarly, in case (c), due to angle $N_3\widehat{N_0}N_1$, Eq. 5 can upper bound ϕ' , i.e., $\phi' < \phi$.

In case (d), $\phi' \leq \phi$ can be derived, as to achieve interference-free, $\frac{\phi'}{2} \leq \min\{N_3\widehat{N_0}N_1_{max}, N_0\widehat{N_3}N_2_{max}\}$ stands. The equality holds only when N_1, N_3 are at h_B , and N_2 is at h_L , which is exactly the triangular wave topology.

Based on the above analysis, any other topology following the pattern of case (a), (c), or (d) requires a beam width ϕ' smaller than the given ϕ in the triangular-wave topology to achieve interference-free.

As for case (b), $\frac{\phi'}{2} \leq \theta$ can be easily derived similarly. However, N_3 may be interfered by the reflected signal from N_0 against the ground. Thus, to be interference-free, $\phi' \leq \max\{N'_0\widehat{N_3}N_0, N'_3\widehat{N_0}N_3\}$, where N'_0, N'_3 are the mirror reflections of N_0, N_3 against the ground, respectively. Otherwise, the reflected interference signal is amplified by G_h on both N_0 and N_3 , and its power is significantly larger than the noise level. It can be proved that $N'_3\widehat{N_0}N_3 \leq N'_0\widehat{N_3}N_0$. Thus, assume N_3 is deployed at $h_M \in [h_B, h_L]$,

$$\phi' \leq \arctan(\frac{h_L - h_M}{3d_0}) + \arctan(\frac{h_L + h_M}{3d_0}) \quad (6)$$

In case (b), to have $\phi' < \phi$, the right side of Eq. 6 must be smaller than ϕ . Using Taylor Expansion, we have,

$$\frac{h_L - 2h_B}{3} - \frac{(h_L - h_B)^3}{d_0^2} > 0 \quad (7)$$

Applying $d_0 = ah_L$, $h_L = bh_B$, Eq. 7 can be further processed, and the relationship in Eq. 4 can be derived. \square

Given d_0 , h_L , and ϕ , selecting h_B to have $\gamma_1 = \frac{\phi}{2}$ leads to the maximum throughput achievable by the triangular wave topology, due to the achieved minimum link length. As an example, assume h_L is 12 m, d_0 is 40 m, and $a = 3.33$. If $\phi = 15^\circ$, $\theta = 11.3^\circ$, and thus $h_B = 4$ m. Since $b = 3 > 2$, $a > \sqrt{\frac{3(b-1)^3}{b^2(b-2)}} = 1.63$, based on Theorem 3, the triangular wave topology offers the optimal throughput among all possible topologies in this setting.

V. NUMERICAL RESULTS AND SIMULATIONS

In this section, numerical and simulation results are provided to show the performance of our proposed schemes and to verify our mathematical analyses.

All evaluations are done at 60 GHz with a 2.16 GHz bandwidth. The transmit power of each wireless node is 1 watt and the antenna gains are $G_h = 21.87$ dBi (generated from Matlab using 16 element circular panel array antenna) and $G_l = 0$ dBi. The pathloss exponent is 2 in the Friis pathloss model used, the attenuation due to oxygen absorption is 16 dB/km, and the reflection attenuation against the ground is 15

dB. We also consider a 15 dB link margin which covers the noise figure and rain attenuation.

In this paper, we focus on deployment along a straight-line highway, or a near straight-line scenario with a slight curve and/or surface height variation due to the practical terrain. As for a specific road trajectory with circles, sharp curves, etc., it would likely need a customized backhaul design to control mutual interference and is outside the scope of this paper.

A. The impact of d_0 and ϕ on BS-to-BS throughput

Assuming that all antennas have a common beam width ϕ , this evaluation shows the trend of BS-to-BS throughput as the distance, d_0 , between two relays increases. A 3 km straight line highway segment with a flat road surface and lampposts evenly deployed is considered. The data from [14] is used where h_L is 15.3 m. h_B is set to 3.0 m. A freeway with 6 lanes and a total width of 22.2 m is considered. The range of d_0 considered is within [30, 1000] m, and d_0 is an integer times the distance between two adjacent lampposts d_L . Typically, d_L is within [30, 100] m. If $d_0 > d_L$, relays are deployed every several lampposts.

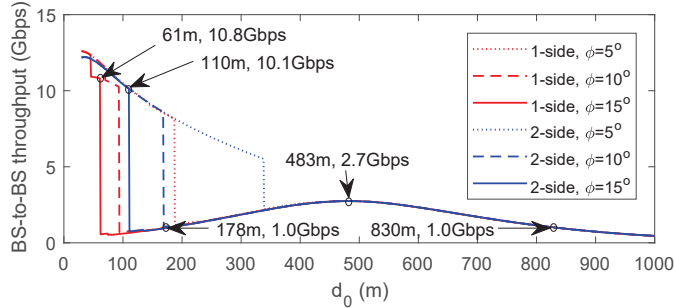


Fig. 8. Throughput vs. d_0

As shown in Fig. 8, for beam width $\phi = 15^\circ$, the BS-to-BS throughput is above 10 Gbps when $d_0 \leq 61$ for the one-side case and when $d_0 \leq 110$ for the two sides case. If d_0 increases beyond this threshold, then the throughput drops substantially to below 1 Gbps, because as d_0 increases, the elevation angle θ decreases given fixed span w as shown in Fig. 3 and Fig. 4. When θ is small enough, Eq. 3 does not hold, and the significant mutual interference reduces the throughput. It is also shown that, the threshold of d_0 to eliminate interference increases when the beam width decreases, which is consistent with Theorem 3.

An interesting phenomenon in Fig. 8 is, after the severe drop due to mutual interference, the throughput gradually increases as d_0 further increases, and it reaches a local maximum of 2.7 Gbps when d_0 is 483m, while after that, the throughput decreases again gradually. This is because due to the use of “by-2” scheduling, the propagation distance of the interference signal increases 3 times faster than d_0 , which means the impact of interference on the throughput is alleviated until interference becomes small enough and the system becomes noise-limited.

These data show that as the BS-to-BS throughput requirement varies, as discussed in Section III-A, the network topology can use different d_0 values and can therefore adapt the

number of relays in between different BS pairs. For example, with $\phi = 5^\circ$ and the two-sides deployment, d_0 can smoothly vary as the BS-to-BS throughput requirement varies between 6 Gbps and 12 Gbps, meaning that the number of relays can be varied from about 3 (at 6 Gbps) to about 20 (at 12 Gbps), assuming BSs are placed every 1 km. Three relays are necessary down to about 2.7 Gbps and then 2 relays are sufficient at that throughput and below. If base stations are spaced around every 800 meters and the throughput requirement is 1 Gbps or less, then no relays are necessary at all.

B. The performance of mmWave backhaul deployment based on real highway data

In practice, the road may not be a perfectly straight line. Thus, in this evaluation, we conduct simulations where the proposed mmWave backhaul network is deployed based on real highway data. To carry out this evaluation, we extracted the lamppost locations in a 12 km segment of highway I-75/85 going through downtown Atlanta, GA from Google Earth. There are 291 lampposts deployed in the median of the highway, which separates the two directions of traffic on the road. Thus, this scenario corresponds to the one-side deployment case in our framework. The average lamppost interval is 41.4 m with a standard deviation σ of 3.32 m and the height h_L of lampposts deployed in Atlanta is about 12 m. Using this real data, we investigate the performance of the triangular-wave topology in non-ideal scenarios.

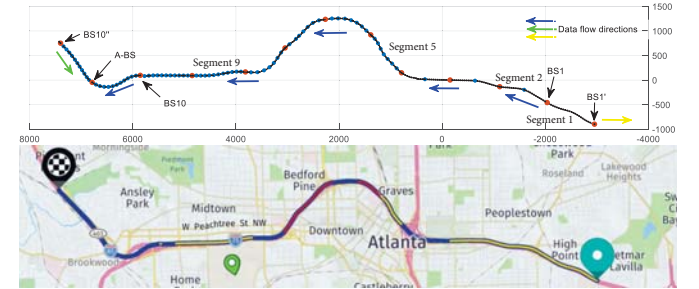


Fig. 9. The modeled segment of highway I75/85 in Atlanta, GA

In the portion of Fig. 9 above the map, the location of each lamppost is marked with a small black circle. We deploy 13 BSs at the locations marked with red dots, achieving a distance between adjacent BSs of about 1 km. The 12 segments have a mean length of 1000.5 m and $\sigma = 19.21$ m. The BS second to the left in Fig. 9 is assumed to be an anchored BS with a fiber backhaul connection, while the other BSs do not have any wired connection. BS1 is the farthest BS associated with this A-BS. We additionally deploy BS10'' on the left end which is associated with this A-BS and BS1' on the right end is a BS associated with a different A-BS. The arrows indicate data flow direction for each BS. It is observed that, despite the fact that the highway segment already includes a significant curve, the deployment of BSs partitions the topology into close-to-straight-line segments. This observation supports our use of a straight-line road model in the analytical evaluations.

We first simulate the self-backhaul design as mentioned in the related work, where BSs connect to each other directly in a

linear topology. Even though this topology should experience interference due to the linear topology, the long distances involved cause each backhaul link to be noise-limited to a rate of around 0.4 Gbps. Thus, narrowing the beamwidth to reduce the interference footprint does not affect the results, as shown in Fig. 10a. Clearly, this topology is not sufficient to meet 5G backhaul requirements. In addition, this result is generated assuming that there is a LOS path between each pair of adjacent BSs. However, due to the existence of obstacles (buildings, tunnels, etc.) alongside the road, the LOS path may be blocked if there is a large curve and this would lead to the total failure of the self-backhaul network.

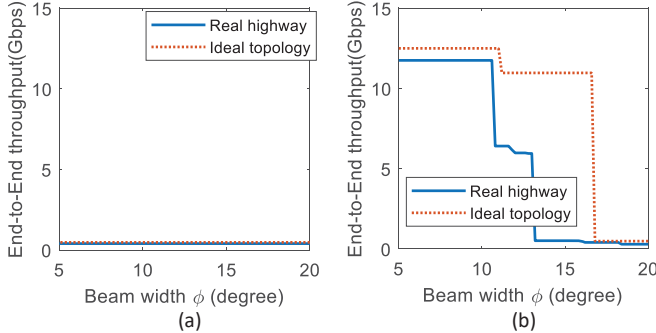


Fig. 10. Comparison on throughput between real topology and ideal topology. (a) Self-backhaul; (b) Backhaul with the maximum number of relays deployed.

Next, we investigate the end-to-end throughput for the triangular-wave topology on the same highway segment with a relay deployed on every lamppost. A comparison between this real road scenario and the ideal scenario is also conducted. As shown in Fig. 10b, when the beamwidth is larger than 17° , both cases have very bad throughput, due to the large mutual interference. When the beamwidth is no larger than 10.6° , both cases have high throughput, 11.77 Gbps and 12.5 Gbps for the real deployment and the ideal deployment, respectively. Between these two thresholds of beamwidth, the throughputs decrease in both cases as the beamwidth increases. We simulated the real road scenario on each segment, and the result of the “worst” segment which provides the worst throughput performance is shown in Fig. 10b. The performance on the real highway scenario is worse than for the ideal case, because the by-2 schedule is not perfect since the non-ideal topology is not perfectly symmetric and there are several long links (the maximum interlamppost separation is 52.8 m).

As mentioned in Section III-A, there is no need for every BS-to-BS connection in the backhaul network to achieve more than 10 Gbps data rate, especially for those connections far away from an anchor BS. From the perspective of reducing the number of relays to control the cost, it is intuitive to think that for connection with a lower rate required, relays can be deployed further apart (every several lampposts). Thus, on the highway segment of Fig. 9, we simulate the deployment of different triangular-wave topologies between different BS pairs using as few relays as possible. The result in Fig. 11 shows that when the antenna beam width $\phi = 5^\circ$, deploying 64 relays between BS1 and A-BS as blue dots depicted in Fig. 9 can satisfy the throughput demands from segment 2 to 11. This is

significantly smaller than the 232 relays that would be used if a relay were deployed on every lamppost. The maximum throughput in Fig. 11 is slightly lower than that in Fig. 10b, because we deploy relays every two lampposts here which corresponds to relatively longer link lengths. Note that no relay is deployed on segment 1 since no data needs to flow between BS1' and BS1.

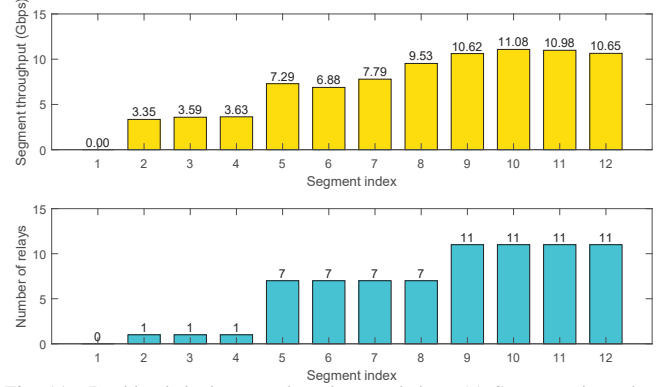


Fig. 11. Backhaul deployment based on real data. (a) Segment throughput; (b) Number of relays in each segment.

ACKNOWLEDGMENT

This research was supported in part by the U.S. National Science Foundation through Award CNS-1513884.

REFERENCES

- [1] Niu, Yong, et al. “A survey of millimeter wave communications (mmWave) for 5G: opportunities and challenges,” *Wireless Networks*, 21.8 (2015): 2657-2676.
- [2] T.L. Frey, “The effects of the atmosphere and weather on the performance of a mmWave communication link,” *Applied Microwave and Wireless*, Vol. 11, pp. 76–81, 1999.
- [3] Zhu, Yibo, et al., “Demystifying 60GHz outdoor picocells,” *Proc. MOBICOM*, pp. 5-16 ACM, 2014.
- [4] Taori, Rakesh, and Arun Sridharan, “Point-to-multipoint in-band mmwave backhaul for 5G networks,” *IEEE Communications Magazine*, 53.1 (2015): 195-201.
- [5] Singh, Sarabjot, et al., “Tractable model for rate in self-backhauled millimeter wave cellular networks,” *IEEE Journal on Selected Areas in Communications*, 33.10 (2015): 2196-2211.
- [6] Zhu, Yun, et al., “QoS-aware scheduling for small cell millimeter wave mesh backhaul,” *Proc. ICC IEEE*, 2016.
- [7] Du, Jinfeng, et al., “Gbps user rates using mmwave relayed backhaul with high-gain antennas,” *IEEE Journal on Selected Areas in Communications*, 35.6 (2017): 1363-1372.
- [8] Zheng, Guanbo, et al., “Toward robust relay placement in 60 GHz mmWave wireless personal area networks with directional antennas,” *IEEE Transactions on Mobile Computing*, 15.3 (2016): 762-773.
- [9] Lan, Zhou, et al., “Directional relay with spatial time slot scheduling for mmWave WPAN systems,” *Proc. Vehicular Technology Conference, IEEE*, 2010.
- [10] Niu, Yong, et al., “Blockage robust and efficient scheduling for directional mmWave WPANs,” *IEEE Transactions on Vehicular Technology*, 64.2 (2015): 728-742.
- [11] Biswas, Sudip, et al., “On the performance of relay aided millimeter wave networks,” *IEEE Journal of Selected Topics in Signal Processing*, 10.3 (2016): 576-588.
- [12] Hu, Qiang and Douglas M. Blough, “Relay selection and scheduling for millimeter wave backhaul in urban environments,” *Proc. IEEE Int'l Conf. on Mobile Ad-hoc and Sensor Systems*, IEEE, 2017.
- [13] Violette, Edmond J., et al., “Millimeter-wave propagation at street level in an urban environment,” *IEEE Transactions on Geoscience and Remote Sensing*, 26.3 (1988): 368-380.
- [14] Lopez, C., “Highway illumination manual,” Austin, TX: Texas Department of Transportation-Traffic Operations Division (2003).